Elastic strain relaxation in GaN/AlN nanowire superlattice

O. Landré,[1] D. Camacho,[2] C. Bougerol,[1] Y. M. Niquet,[2] V. Favre-Nicolin,[3] G. Renaud,[4] H. Renevier,[5] and B. Daudin[1]

[1]*CEA-CNRS Group "Nanophysique et Semiconducteurs," Institut Néel/CNRS–Univ. J. Fourier and CEA, INAC, SP2M,*
17 rue des Martyrs, 38 054 Grenoble, France

[2]*CEA, INAC, SP2M, L_Sim, 17 rue des Martyrs, 38 054 Grenoble Cedex 9, France*

[3]*Joseph Fourier University and CEA, INAC, SP2M, L-NRS, 17, rue des Martyrs, 38054 Grenoble Cedex 9, France*

[4]*CEA, INAC, SP2M, L-NRS, 17, rue des Martyrs, 38054 Grenoble Cedex 9, France*

[5]*Laboratoire des Matériaux et du Génie Physique, Grenoble INP-MINATEC, 3 parvis L. Néel, 38016 Grenoble*

The molecular-beam epitaxy growth of AlN/GaN nanowire superlattices has been studied by using a combination of *in situ* x-ray diffraction experiments, high-resolution electron-microscopy analysis and theoretical calculations performed in a valence force field approach. It is found that the nanowire superlattices are in elastic equilibrium, in contrast with the two-dimensional case but in line with the predicted increase in the critical thickness in the nanowire geometry.

PACS number(s): 61.46.Km, 81.05.Ea, 81.15.Hi, 61.05.cp

Accurate prediction of the optical properties of nitride heterostructures requires an in-depth understanding of their strain-relaxation mechanisms, due to the presence of the strain-sensitive internal electric field, a combination of both spontaneous polarization and piezoelectric components. In the case of two-dimensional (2D) GaN/AlN superlattices, it has been established that strain relaxation relies on the granular growth mode of nitrides, which leads to the formation of edge dislocations at the coalescence between adjacent grains.[1] It has actually been pointed out that the average in-plane lattice parameter a of such superlattices is not the one expected from a purely elastic behavior as an evidence for dislocation formation.[2] More generally, in the case of thick layers of GaN or AlN, it has been shown that strain relaxation is of plastic nature and occurs by formation of nonmobile edge dislocations, leading to a strain gradient in the layers.[3]

By contrast nanowires (NWs) of GaN can be considered as an assembly of perfect, noncoalesced, vertically elongated grains. Their large height/diameter aspect ratio is expected to favor elastic-strain relaxation, making them virtually free of dislocations, consistent with their excellent optical properties.[4] Then, one can wonder whether strain relaxation is also purely elastic in GaN/AlN NW heterostructures, at variance with their 2D counterpart. It is the goal of the present Brief Report to address this issue by a combination of *in situ* x-ray diffraction (XRD) experiments, high-resolution transmission electron microscopy (HRTEM) and theoretical calculations on GaN/AlN NW superlattices.

In situ grazing incidence x-ray diffraction experiments were performed at the BM32 beamline of the European Synchrotron Radiation Facility (ESRF) in Grenoble (France). The substrate consisted of (111) Si. After standard degreasing and deoxidation by dipping in hydrofluoric acid, it was introduced in an on-line versatile molecular-beam-epitaxy (MBE) chamber equipped with Ga and Al effusion cells and with a N radio-frequency plasma cell to produce active N. A thin AlN buffer layer (about 2–3-nm thick) was deposited in Al-rich conditions onto the (111) Si substrate. Due to the coincidence relationship between in-plane AlN and Si(111) lattice parameter (five interplanar AlN distances correspond-

ing to four interplanar distances in Si), and to the relatively small in-plane lattice mismatch between AlN and GaN (about 2.4 %), such a buffer layer results in GaN NWs oriented perpendicular to the substrate surface.[5] These GaN NWs were used as a base for the growth of the AlN/GaN superlattice. Standard conditions were used for NW growth, namely, strongly N-rich conditions (metal/N ratio of about 0.3) and a growth temperature in the 800–850 °C range.[5] The height of the GaN NW base was chosen large enough (>200 nm) to relieve any strain induced at the interface with the buffer, given the typical diameter of such nanowires (~ 25 nm). The growth of the AlN buffer layer, the GaN NW base, and the GaN/AlN superlattice subsequently deposited was studied by performing h scans along the $[10\bar{1}0]$ direction in the reciprocal space near the in-plane AlN $(30\bar{3}0)$ reflection (radial scans are sensitive to strain). The x-ray beam energy was 10260 eV. The scattered signal was recorded at grazing angles ($\alpha_i = 0.15°$) with a Vantec™ linear detector.[6] Note that in the following the reciprocal lattice unit h refers to the Si reciprocal space. The latter is obtained for Si described in a hexagonal cell whose [0001] direction is parallel to the cubic [111] axis. The hexagonal cell parameters are therefore $a_{h,Si} = \sqrt{2}/2a_{c,Si}$ and $c_{h,Si} = \sqrt{3}a_{c,Si}$, where $a_{c,Si}$ is the lattice parameter of the Si cubic cell. This means that the room-temperature h value corresponding to the $(30\bar{3}0)$ reflection of bulk AlN and bulk GaN are equal to 3.706 and 3.62, respectively.

Online monitoring of the GaN/AlN superlattice growth is shown in Fig. 1(a). The diffraction peak at $h = 3.605$ corresponds to the GaN NW base. The peak shift with respect to room temperature value (at $h = 3.62$) is consistent with the expected thermal expansion of GaN,[7,8] as the NW growth was performed in the 800–850 °C temperature range. The diffraction peaks near $h = 3.65$ correspond to the step-by-step deposition of the GaN/AlN NW superlattice.

In order to gain more insight into the evolution of the GaN/AlN NW superlattice strain state, calculations were made using Keating's valence force field (VFF) model, which provides an atomistic description of the elasticity of tetrahedrally bonded semiconductors. The original VFF (Ref.
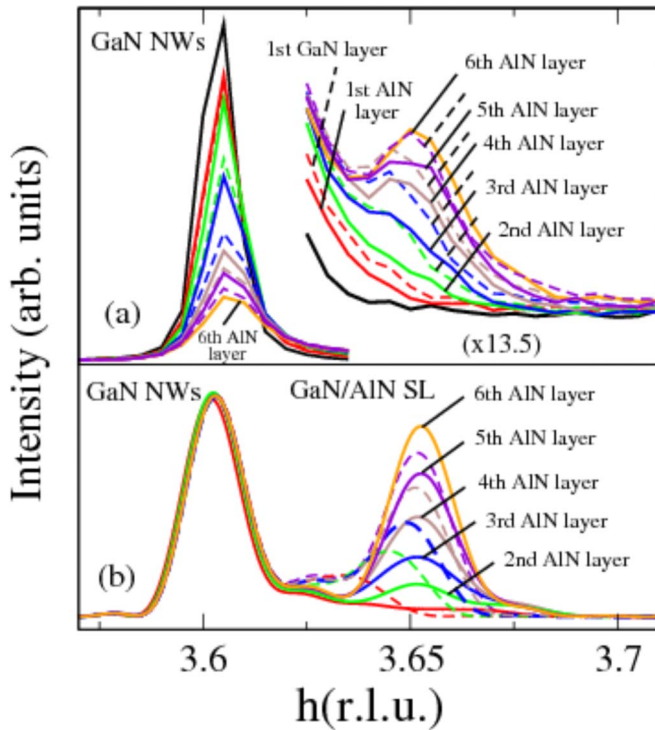
FIG. 1. (Color online) (a) Sets of h scans (radial scans) near the in-plane GaN $(30\bar{3}0)$ reflection, indexed in the Si hexagonal cell, taken at different steps of the AlN/GaN NW superlattice deposition. The x-ray beam incidence angle is 0.15° and the energy 10260 eV. The AlN (respectively, GaN) critical angle at this energy is 0.21° (respectively, 0.26°). (b) X-ray diffraction peaks calculated from the atomic positions computed in a purely elastic model (valence force field approach). Relaxed AlN XRD peak (at 825 °C), if present, is expected at $h \sim 3.69$.

9) was modified to account for the different bond lengths and bond angles in the wurtzite structure.[10] The lattice parameters a and c of GaN and AlN at the growth temperature $T \approx 825$ °C are taken from Refs. 7 and 8. The bond-stretching and bond-bending constants of the VFF were fitted to the macroscopic elastic constants C_{ij} extrapolated at $T = 825$ °C.[11] The nanocolumns were modeled as 23-nm-diameter and 100-nm-long GaN pillars with the AlN/GaN heterostructure on top. The diameter of the NWs (23 nm) as well as the thickness of the AlN and GaN layers in the superlattice, namely, 2.3 and 2 nm, respectively, were extracted from HRTEM measurements described below in details. Up to six AlN and five GaN layers were added one at a time. For each layer, the structure was relaxed with the VFF and the scattered x-ray amplitude was computed from the atomic positions using the kinematical approximation around the AlN and GaN $(30\bar{3}0)$ reflection [i.e., h in the range of 3.55–3.70 in the Si(111) reciprocal lattice units]. For each h value, the intensity was integrated over the outgoing angle between 0° and 2.5° corresponding to the actual detector angular acceptance. Note that only the upper 20 nm of the GaN pillars were taken into consideration for convenience, in order to make the diffraction peak intensity of the GaN pillar and superlattice comparable. Results of the calculation are shown in Fig. 1(b). Both the GaN pillar and the superlattice diffrac-

tion peaks are slightly shifted toward small h values with respect to the experimental data due to the uncertainty in determining the real-growth temperature. However, this corresponds to a 0.02 % discrepancy in the in-plane strains, which is negligible with respect to the 2.4 % lattice mismatch between AlN and GaN. Despite this shift indicating that the actual-growth temperature was slightly lower than expected, calculations exhibit an excellent agreement with the experimental data reported in Fig. 1(a). In particular, the diffraction peak computed after the addition of a new GaN layer progressively shifts to higher h values while the diffraction peak computed after the addition of a new AlN layer emerges almost straight at $h \sim 3.655$. The motion of the peaks rapidly fades as the inner layers of the superlattice almost end in elastic equilibrium with the *average* alloy (45% GaN-55% AlN) suggested by the nominal thicknesses of GaN and AlN layers, thanks to the efficient strain relaxation of the superlattice allowed by the free surfaces. These trends are very well reproduced by the experimental data, as a first clue that the GaN/AlN NW superlattice is in elastic equilibrium with the GaN base.

At this stage, it has to be emphasized that due to the reduced NW diameter, the presence of a single misfit dislocation at an AlN/GaN interface would lead to a significant relaxation of the 2.4% in-plane lattice mismatch between AlN and GaN. If this was repeated for each AlN and GaN layer of the superlattice, as in the 2D case,[1,2] one would not expect a single diffraction peak at the average alloy position, in contradiction with the actual experimental observations.

We have, moreover, performed additional calculations (not shown here) on nanowires with a $\sim 50\%$ larger diameter (30 nm). The peak positions are almost unchanged in the XRD pattern while their width is only slightly decreased due to size effects as an evidence that NW diameter distribution effects can be neglected.

HRTEM and HR-STEM experiments on the same sample as described above were performed using a Jeol 4000EX microscope operated at 400 kV (Cs=1 mm) and a FEI Titan having a Cs probe corrector operated at 300 kV, respectively. For that purpose a cross-sectional specimen was prepared by sandwiching a slice of the NW sample together with a Si one using epoxy, and mechanically thinning the region of interest. The sample was then ion milled to electron transparency using a Gatan PIPS equipment. The HRTEM image taken along the $[11\bar{2}0]$ zone axis and given in Fig. 2(a) shows the top part of a typical NW (23 nm in diameter), consisting in a GaN pillar (dark contrast), followed by five 2 nm thick GaN inclusions separated by 2.3 nm thick AlN spacers (light contrast). The high-angle angular dark-field (HAADF) image (HR-STEM mode) shown in Fig. 2(b) clearly reveals the absence of significant interdiffusion at the interfaces between AlN (dark) and GaN (light). In order to increase the image contrast and the signal-to-noise ratio in view of performing a strain analysis with the geometrical phase method,[12] the sample was then tilted by about 10° around the c^* reciprocal axis.[13] The (0002) reflection was selected in the Fourier transform to obtain the map of the c lattice parameter of the NW. The reference region was chosen as the GaN pillar below the superlattice with $c_{ref} = c_{GaN \, bulk} = 0.5185$ nm. A profile
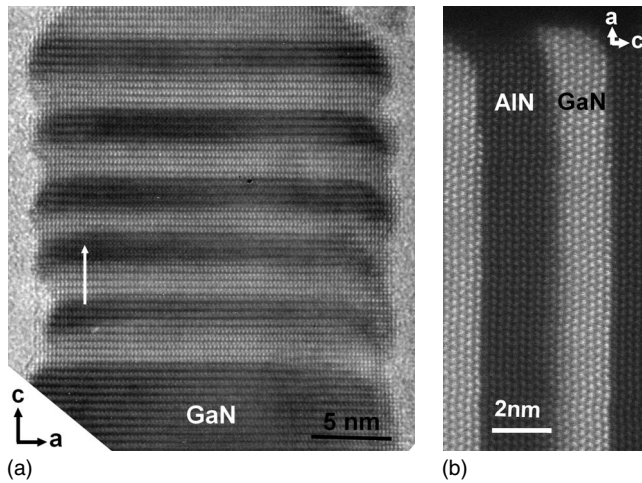
FIG. 2. (a) HRTEM image of the NW GaN/AlN superlattice. Five AlN/GaN bilayers grown on a GaN basis are visible. The arrow indicates growth direction. (b) HAADF image showing that no significant interdiffusion occurs between AlN and GaN

of c along the growth axis integrated over a 7-nm-wide region in the central part of the NW is given in Fig. 3(a).

In order to make a comparison with HRTEM results, the local c parameter was computed with Keating's VFF from the average projections of the atomic columns perpendicular to the wire (see Ref. 14) using room-temperature GaN and AlN lattice parameters. The result, shown in Fig. 3(b), puts in evidence an increase in c in the GaN insertions with respect to c_{ref}, which is in satisfactory agreement with the HRTEM profile. It can be noticed that this c value (0.522 nm), if introduced in the Poisson formula, leads to an in-plane parameter $a = 0.315$ nm, corresponding to the value of a 55% AlN-45% GaN alloy, i.e., also consistent with the nominal composition expected from the thickness of the AlN and GaN layers in the NW superlattice.

The agreement between the experiments reported above and the calculation performed in the framework of a purely elastic model is consistent with the fact that no dislocations could be identified in Fig. 2 at the interface between AlN and GaN. This further supports the conclusion that the GaN/AlN NW superlattice is in elastic equilibrium with the GaN base. More generally, the issue of the critical thickness in axial NW heterostructures has been theoretically addressed by Ertekin *et al.*[15] and by Glas.[16] These authors have used a thermodynamical approach based on the classical model of Mattews for the determination of the critical thickness in 2D heterolayers.[17] They find that the critical thickness is far larger in nanowires than in 2D heterostructures thanks to the additional relaxation allowed by the NW free surfaces. In particular, they both predict the existence of a critical radius below which an infinitely long circular section can be grown on a mismatched basis. The value of the critical radius was found to depend on the lattice mismatch between the two segments as well as on the type and the Burgers' vector value of the dislocations introduced to minimize the total elastic energy. Although a precise determination of the critical thickness of axial NW heterostructures should take into account their exact hexagonally faceted shape and consider the
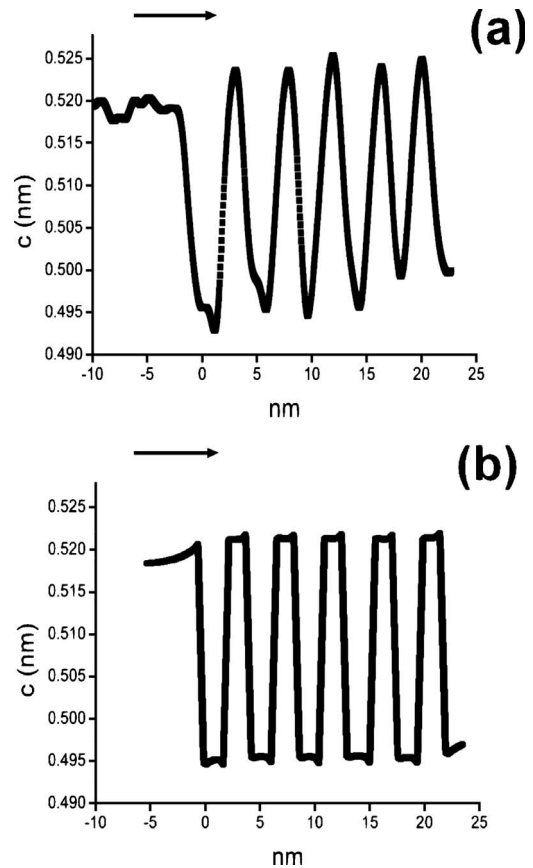
FIG. 3. (a) Profile of the c parameter, along the growth axis and taken in the central part of a NW, obtained from the geometrical phase analysis of the HRTEM image. The arrows indicate growth direction. For convenience, the x-axis origin has been taken as the top of GaN pillar basis before the growth of the first AlN layer. (b) Profile of the c parameter computed with Keating's valence force field.

kinetical aspects of dislocation formation, the above-mentioned theoretical approach was found to realistically predict the critical radius for various experimental systems.[16] In the present case, an extrapolation of the theoretical data to GaN/AlN, assuming the formation of misfit dislocations with a Burgers' vector in the 0.1–0.3-nm range, leads to a critical radius of about 10–30 nm, respectively (Ref. 15). Although the radius (11 nm) of the heterostructures considered here lays in the lower limit of this range, the experimental data are clearly consistent with a purely elastic-strain-relaxation mechanism. This further emphasizes the potential of NWs for the growth of dislocation-free superlattices. As it was recently reported, the quantum-confined Stark effect governing the optical properties of GaN insertions in AlN NWs is found to be significantly reduced with respect to the 2D GaN case.[18] Consistent with the results reported in the present work, this may be assigned to the reduction in the piezoelectric component of the internal electric field, as a consequence of the efficient elastic-strain relaxation in the NW geometry. Whereas it is now well established that the diameter of catalyst-free GaN NWs grown by plasma-assisted MBE is typically in the 20–50-nm range, it has been recently dem-

onstrated that this also holds in the case of AlN NWs.[19] Therefore it can be safely concluded that the results reported here for the 2.4 % lattice mismatched AlN/GaN model system should also hold *a fortiori* for AlGaN/GaN or AlGaN/AlN heterostructures in the whole composition range, opening the path to the control of their growth and to the understanding of their optical properties.

[1] A. Bourret, C. Adelmann, B. Daudin, J.-L. Rouvière, G. Feuillet, and G. Mula Phys. Rev. B **63**, 245307 (2001).

[2] P. K. Kandaswamy, F. Guillot, E. Bellet-Amalric, E. Monroy, L. Nevou, M. Tchernycheva, A. Michon, F. H. Julien, E. Baumann, F. R. Giorgetta, D. Hofstetter, T. Remmele, M. Albrecht, S. Birner, and L. S. Dang, J. Appl. Phys. **104**, 093501 (2008).

[3] E. Bellet-Amalric, C. Adelmann, E. Sarigiannidou, J. L. Rouvière, G. Feuillet, E. Monroy, and B. Daudin, J. Appl. Phys. **95**, 1127 (2004).

[4] E. Calleja, M. A. Sanchez-Garcia, F. J. Sanchez, F. Calle, F. B. Naranjo, E. Muñoz, U. Jahn, and K. Ploog, Phys. Rev. B **62**, 16826 (2000).

[5] R. Songmuang, O. Landré, and B. Daudin, Appl. Phys. Lett. **91**, 251902 (2007).

[6] J. Coraux, H. Renevier, V. Favre-Nicolin, G. Renaud, and B. Daudin, Appl. Phys. Lett. **88**, 153125 (2006).

[7] C. Roder, S. Einfeldt, S. Figge, and D. Hommel, Phys. Rev. B **72**, 085218 (2005).

[8] S. Figge, H. Kröncke, D. Hommel, and B. M. Epelbaum, Appl. Phys. Lett. **94**, 101915 (2009).

[9] P. N. Keating, Phys. Rev. **145**, 637 (1966).

[10] D. Camacho and Y. M. Niquet, Physica E **42**, 1361 (2010).

[11] R. R. Reeber and K. Wang, MRS Internet J. Nitride Semicond. Res. **6**, 3 (2001).

[12] M. Hÿtch, E. Snoeck, and R. Kilaas, Ultramicroscopy **74**, 131 (1998).

[13] J. L. Rouvière, P. Bayle-Guillemaud, G. Radtke, S. Groh, and O. Briot, Inst. Phys. Conf. Ser. **169**, 17 (2001); E. Sarigianni-dou, A. D. Andreev, E. Monroy, B. Daudin, and J. L. Rouvière, Phys. Status Solidi C **3**, 1667 (2006).

[14] C. Bougerol, R. Songmuang, D. Camacho, Y. M. Niquet, R. Mata, A. Cros, and B. Daudin, Nanotechnology **20**, 295706 (2009).

[15] E. Ertekin, P. A. Greaney, D. C. Chrzan, and T. D. Sands, J. Appl. Phys. **97**, 114325 (2005).

[16] F. Glas Phys. Rev. B **74** 121302(R) (2006).

[17] J. W. Matthews and A. E. Blakeslee, J. Cryst. Growth **27**, 118 (1974).

[18] J. Renard, R. Songmuang, G. Tourbot, C. Bougerol, B. Daudin, and B. Gayral, Phys. Rev. B **80**, 121305(R) (2009).

[19] O. Landré, V. Fellmann, P. Jaffrennou, C. Bougerol, H. Renevier, A. Cros, and B. Daudin, Appl. Phys. Lett. **96**, 061912 (2010).